

# Direct Delivery of Antisense Oligonucleotides to the Middle and Inner Ear Improves Hearing and Balance in Usher Mice

Jennifer J. Lentz,<sup>1,2,7</sup> Bifeng Pan,<sup>3,7</sup> Abhilash Ponnath,<sup>1,7</sup> Christopher M. Tran,<sup>1</sup> Carl Nist-Lund,<sup>3</sup> Alice Galvin,<sup>3</sup> Hannah Goldberg,<sup>3</sup> Katelyn N. Robillard,<sup>2</sup> Francine M. Jodelka,<sup>4</sup> Hamilton E. Farris,<sup>1,2</sup> Jun Huang,<sup>5</sup> Tianwen Chen,<sup>5</sup> Hong Zhu,<sup>5</sup> Wu Zhou,<sup>5</sup> Frank Rigo,<sup>6</sup> Michelle L. Hastings,<sup>4</sup> and Gwenaëlle S.G. Géléoc<sup>3</sup>

<sup>1</sup>Department of Otorhinolaryngology, Louisiana State University Health Sciences Center, New Orleans, LA 70112, USA; <sup>2</sup>Neuroscience Center of Excellence, Louisiana State University Health Sciences Center, New Orleans, LA 70112, USA; <sup>3</sup>Department of Otolaryngology, Boston Children's Hospital, Harvard Medical School, Boston, MA 02115, USA; <sup>4</sup>Center for Genetic Diseases, Chicago Medical School, Rosalind Franklin University of Medicine and Science, North Chicago, IL 60064, USA; <sup>5</sup>Department of Otolaryngology and Communicative Sciences, University of Mississippi Medical Center, Jackson, MS 39216, USA; <sup>6</sup>Ionis Pharmaceuticals, Inc., Carlsbad, CA 92008, USA

**Usher syndrome is a syndromic form of hereditary hearing impairment that includes sensorineural hearing loss and delayed-onset retinitis pigmentosa (RP). Type 1 Usher syndrome (USH1) is characterized by congenital profound sensorineural hearing impairment and vestibular areflexia, with adolescent-onset RP. Systemic treatment with antisense oligonucleotides (ASOs) targeting the human *USH1C* c.216G>A splicing mutation in a knockin mouse model of USH1 restores hearing and balance. Herein, we explore the effect of delivering ASOs locally to the ear to treat hearing and vestibular dysfunction associated with Usher syndrome. Three localized delivery strategies were investigated in *USH1C* mice: inner ear injection, trans-tympanic membrane injection, and topical tympanic membrane application. We demonstrate, for the first time, that ASOs delivered directly to the ear correct *Ush1c* expression in inner ear tissue, improve cochlear hair cell transduction currents, restore vestibular afferent irregularity, spontaneous firing rate, and sensitivity to head rotation, and successfully recover hearing thresholds and balance behaviors in *USH1C* mice. We conclude that local delivery of ASOs to the middle and inner ear reach hair cells and can rescue both hearing and balance. These results also demonstrate the therapeutic potential of ASOs to treat hearing and balance deficits associated with Usher syndrome and other ear diseases.**

## INTRODUCTION

Usher syndrome is a rare genetic disease that affects 1 in 20,000 individuals worldwide<sup>1,2</sup> and is associated with concurrent hearing loss and retinitis pigmentosa (RP), leading to progressive loss of vision. Eleven genes and three clinical subtypes (USH1, USH2, and USH3) are associated with the disease. Patients with USH1, the most severe form, suffer from severe to profound hearing impairment at birth, balance deficits, and early adolescent-onset of RP. Six genes (*MYO7A* [USH1B], *USH1C* [USH1C], *CDH23* [USH1D], *PCDH15* [USH1F], *SANS* [USH1G], and *CIB2* [USH1J]) are associated with USH1<sup>3</sup> that encode

for proteins expressed in inner ear hair cells and retinal photoreceptor cells. These proteins are involved in the development, maturation, and function of the sensory cells.<sup>4–8</sup>

The *USH1C* gene, encoding the scaffolding protein harmonin, was identified by linkage analysis of Acadian families in southwestern Louisiana.<sup>9–11</sup> A splicing mutation (c.216G>A) in exon 3 of the *USH1C* gene was later identified to cause a 35-bp deletion in the mRNA transcript that leads to expression of a truncated harmonin at the expense of the wild-type (WT) protein.<sup>12</sup> Mice engineered to contain the human c.216G>A mutation (*Ush1c*<sup>216AA</sup>) also have profound hearing loss, balance deficits, and visual impairments similar to patients.<sup>13,14</sup> Recently, two different genetic strategies were tested to restore hearing and balance in *Ush1c*<sup>216AA</sup> mice. The first demonstrates successful recovery of auditory and balance function following systemic treatment via intraperitoneal (i.p.) injections with a splice-switching antisense oligonucleotide (ASO) targeting the 216A mutation (ASO-29).<sup>15–17</sup> ASOs of this type are short oligonucleotides that base-pair to precursor (pre-)mRNA and create a steric block that modifies downstream RNA processing, such as splicing.<sup>18</sup> In the case of mutations such as c.216G>A that create *de novo* splice sites, ASOs can be designed to block the aberrant *de novo* splice site and redirect splicing to the correct site, thereby restoring RNA processing and expression of functional protein.<sup>19,20</sup> A significant improvement of auditory sensitivity down to ~50 dB (16-kHz stimuli), with the best performers down to ~30 dB, was achieved after i.p. injections of ASO-29 in *Ush1c*<sup>216AA</sup> mice at postnatal day 5 (P5).<sup>15</sup> More

Received 16 April 2020; accepted 2 August 2020;  
<https://doi.org/10.1016/j.ymthe.2020.08.002>.

<sup>7</sup>These authors contributed equally to this work.

**Correspondence:** Jennifer J. Lentz, Department of Otorhinolaryngology, LSUHSC, 2020 Gravier Street, Lions Boulevard, Room 795, New Orleans, LA 70112, USA.

**E-mail:** [jlentz@lsuhsc.edu](mailto:jlentz@lsuhsc.edu)

**Correspondence:** Gwenaëlle S.G. Géléoc, Department of Otolaryngology, Boston Children's Hospital, Harvard Medical School, 3 Blackfan Circle, CLS 03001, Boston, MA 02115-5737, USA.

**E-mail:** [gwenaelle.geleoc@childrens.harvard.edu](mailto:gwenaelle.geleoc@childrens.harvard.edu)

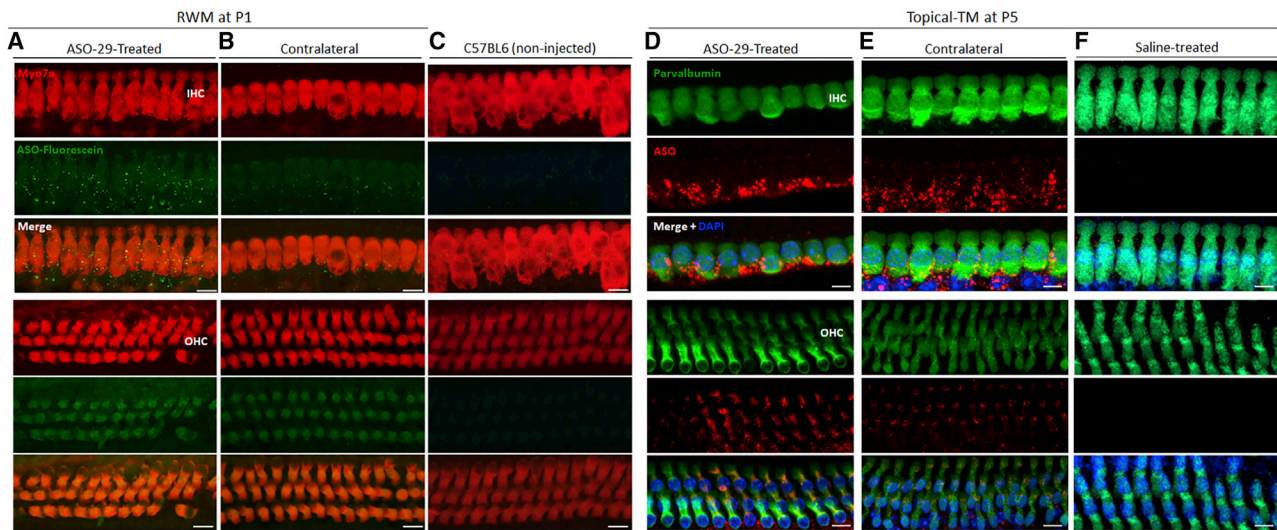


**Figure 1. ASO-29 Localizes to Hair Cells after Delivery through the Round Window and Tympanic Membranes in *Ush1c*<sup>216AA</sup> Mice**

(A–F) Immunohistochemistry analysis of auditory hair cells in the middle turn of the cochlea (1.8–2.2 mm from the apex tip) from 1-month-old *Ush1c*<sup>216AA</sup> mice treated with ASO-29 via (A and B) RWM injection, (D and E) topical-TM application with gel foam, and C57BL6 non-injected (C) or topical-TM saline treated *Ush1c*<sup>216AA</sup> mice (F). (A and B) ASO-29 (30 μg, ASO-29-fluorescein, green) is detected in inner hair cells (IHCs) and outer hair cells (OHCs) (Myo7a, red) from the treated (A) and contralateral (B) ears of *Ush1c*<sup>216AA</sup> mice treated with ASO-29 by RWM injection at P1. (D and E) ASO-29 (100 μg, red) is detected (anti-ASO-29 antibodies) in IHCs and OHCs (parvalbumin, green) from the treated (D) and contralateral (E) ears of *Ush1c*<sup>216AA</sup> mice treated by topical-TM application of ASO-29 with gel foam at P5. No signal is detected in C57BL6 non-injected mice (C) and *Ush1c*<sup>216AA</sup> mice treated by topical-TM application of saline with gel foam at P5. Scale bars indicate 10 μm. RWM, round-window membrane; TM, tympanic membrane; P, postnatal day.

recently, it was shown that earlier ASO-29 treatment at P1 in these mice improved the rescue of auditory sensitivity down to ~32 dB (16-kHz stimuli), demonstrating a window of therapeutic efficacy.<sup>16</sup> In another approach, Pan et al.<sup>21</sup> treated the same mouse model with adeno-associated virus (AAV) vectors driving expression of functional harmonin. They showed that round window membrane (RWM) injections of AAV2/Anc80.CMV.harmonin at P1 also successfully improved auditory function down to ~50 dB and near WT levels for the best performers (25 dB) (16-kHz stimuli). For both the antisense and gene therapy treatments, auditory recovery in *Ush1c*<sup>216AA</sup> mice was associated with increased expression of full-length *Ush1c* mRNA, restoration of functional harmonin protein expression, improvements in stereocilia organization, and survival of cochlear hair cells. Low- to mid-frequency hearing recovery was maintained up to 6 months of age (latest time reported) with both therapies, albeit loss of sensitivity was observed over time.

Clinically, ASOs are desirable in that they target pre-mRNA to correct RNA processing while preserving endogenous regulation of gene expression. Furthermore, commercially approved ASO therapies have been demonstrated to be well tolerated in patients for cytomegalovirus (CMV) retinitis, spinal muscular atrophy (SMA), and Duchenne muscular dystrophy (DMD).<sup>22–24</sup> These treatments use a variety of delivery strategies, including intravitreal injection, intravenous injection, and intrathecal injection to directly target cells in the ocular, nervous, and muscular systems, respectively. In this study, we sought to test the feasibility of delivering ASO-29 directly to the ear for the treatment of hearing and balance dysfunction in Usher mice. Three localized delivery strategies were investigated: RWM in-

jection, topical tympanic membrane (topical-TM) application, and trans-TM injection of ASO-29 in neonatal Usher mice (Figure S1), followed by an analysis of hearing and balance function. While the TM is partially formed in newborn mice covering 20% of its final size, it continues to grow and mature during the first 3 postnatal weeks.<sup>25</sup> Additionally, we found insufficient middle ear space for the injection of 0.5 μL of drug solution before P9. To overcome these developmental structural constraints in the mouse ear, we chose to deliver ASO-29 via topical-TM application at P5 and trans-TM injection at P10 and P20. Using these approaches, we show the presence of ASO-29 in cochlear hair cells after RWM and TM treatments and demonstrate significant improvement of auditory and balance function in treated *Ush1c*<sup>216AA</sup> mice. The recovery is associated with correction of RNA splicing, as well as improved harmonin expression in cochlear hair cell bundles, bundle morphology, and hair cell survival. We conclude that hearing and balance deficits associated with Usher syndrome can be treated with direct middle and inner ear delivery of ASOs targeting cochlear hair cells. These results also demonstrate the potential of using ASOs for the treatment of ear diseases in general.

## RESULTS

### Local Delivery of ASO-29 to the Middle and Inner Ear Targets Hair Cells of the Cochlea

To determine whether localized delivery of ASOs reaches the sensory cells of the inner ear, we assessed the presence of ASO-29 in cochlear hair cells after injection through the RWM at P1 (30 μg of ASO-29-fluorescein) or applied topically with gel foam onto the TM at P5 (ASO-29, 100 μg or saline) in *Ush1c*<sup>216AA</sup> mice (Figure 1).

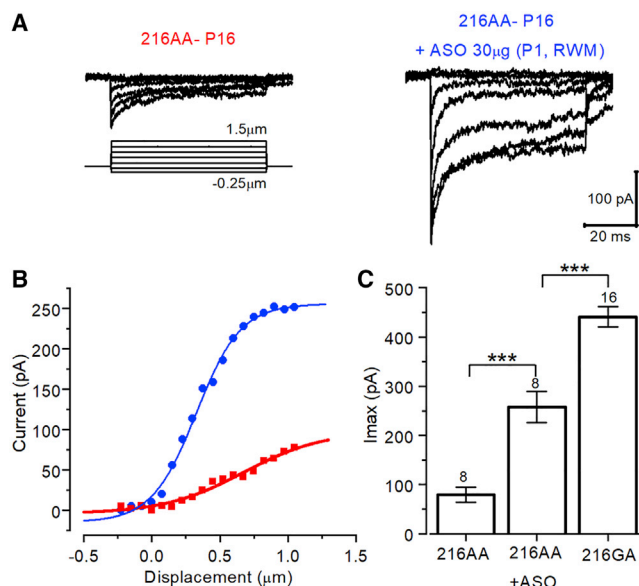


**Figure 2. Round Window Membrane Injection of ASO-29 Improves Hair Cell Mechanosensitivity in Ush1c<sup>216AA</sup> Mice**

MET currents were elicited by square step displacements of the hair bundle in apical IHCs from cultured organs of Corti harvested from Ush1c<sup>216AA</sup> mice treated with ASO-29 at P1 via RWM injection, as well as untreated Ush1c<sup>216AA</sup> mutant and heterozygous (Ush1c<sup>216GA</sup>) control littermates. (A) Representative MET currents recorded from Ush1c<sup>216AA</sup> control (216AA) and ASO-29-treated Ush1c<sup>216AA</sup> mice (216AA+ASO-29, 30 µg). Small MET currents were evoked in IHCs from 216AA control mice, whereas large currents were elicited in IHCs from ASO-29-treated 216AA mice. (B) Corresponding current-displacement curves for MET currents from (A) and (B) show an increase in current after displacement of an IHC bundle from an ASO-29-treated 216AA mouse (blue line) compared with an untreated control mutant (red line). (C) Average maximal MET currents were significantly larger in IHCs of ASO-29-treated 216AA mice ( $p < 0.001$ ) but also significantly smaller than those from 216GA heterozygous mice ( $p < 0.001$ ). Data are represented as mean  $\pm$  SEM. \*\*\* $p < 0.001$  (one-way ANOVA, Prism). P, postnatal day; RWM, round-window membrane.

Tissues from the treated and contralateral untreated ears were harvested for immunohistochemistry at 4 weeks of age. ASO-29 fused to fluorescein was detected in hair cells of the RWM injected ear and to a lesser extent in the contralateral ear (Figures 1A and 1B). ASO-29 was also observed around hair cell bodies, which may be associated with supporting cells. ASO-29 was detected along the entire organ with no significant differences between base, middle turn, and apex. Interestingly, ASO-29-fluorescein could also be detected in utricles of injected Ush1c<sup>216AA</sup> mice (Figure S2). Remarkably, ASO-29 was detected using an anti-ASO antibody in and around hair cells of ASO-treated and contralateral ears after topical-TM application (Figures 1D and 1E). ASO-29 was more prominent in inner hair cells (IHCs) than outer hair cells (OHCs) with both RWM and topical-TM deliveries. The dimer, more diffuse pattern observed in OHCs may indicate different amounts of drug in each cell type, suggesting more internalization of ASO-29 via endosomes in IHCs.

### Local Delivery of ASO-29 to the Inner Ear Rescues Mechano-Electrical Transduction (MET) in Usher Mice

To assess functional hair cell recovery after local ASO-29 treatment, transduction currents were recorded after stiff probe deflections of cultured cochlear IHCs harvested from untreated and ASO-29-treated Ush1c<sup>216AA</sup> mutant and normal hearing littermates. Ush1c<sup>216AA</sup> mice were treated with 30 µg of ASO-29 by RWM injection at P1. The auditory organ was then acutely excised at P6 and maintained in culture for 10 days to allow recovery of WT harmonin expression after ASO-29 treatment. Organs of Corti from untreated Ush1c<sup>216AA</sup> mutant and heterozygous Ush1c<sup>216GA</sup> control mice were also harvested at P6 and maintained in culture for the same duration. MET currents induced by square step displacement of the apical hair bundles were recorded from IHCs of the cultured cochlea. Significantly larger MET currents were recorded in IHCs from Ush1c<sup>216AA</sup> mice treated with ASO-29 by RWM injection ( $p > 0.001$ ; Maximum MET current ( $I_{max}$ ),  $I_{max} = 257 \pm 90$  pA,  $n = 8$ ), compared with IHCs from untreated Ush1c<sup>216AA</sup> mice ( $I_{max} = 80 \pm 43$  pA,  $n = 8$ ) (Figures 2A and 2B). Although MET currents were significantly improved in ASO-29-treated Ush1c<sup>216AA</sup> IHCs, they remained smaller than IHC currents recorded from control heterozygous mice ( $I_{max} = 440 \pm 82$  pA,  $n = 16$ ) (Figure 2C). These results demonstrate that ASO-29 treatment delivered by RWM injection in P1 Ush1c<sup>216AA</sup> mice significantly improved IHC mechanosensitivity.

### Local Delivery of ASO-29 to the Middle and Inner Ear Improves Auditory Sensitivity in Usher Mice

Ush1c<sup>216AA</sup> mice have severe to profound hearing impairment at 1 month of age as evidenced by little/no auditory-evoked brainstem responses (ABRs) or distortion product otoacoustic emissions (DPOAEs) across all frequencies.<sup>14–16,21</sup> ABRs measure the function of auditory IHCs and OHCs, while DPOAEs measure OHC function only, in response to acoustic stimuli. To assess whether a single treatment of ASO-29 delivered locally to the ear improves hearing function, ABRs and DPOAEs were measured in Ush1c<sup>216AA</sup> mice treated with ASO-29, a control ASO (ASO-C), or saline at various developmental ages (Figures 3 and 4). We delivered ASO-29 to the inner ear by RWM injection at P1, applied externally to the TM with gel foam (topical-TM) at P5, or to the middle ear by trans-TM injection at P10 or P20 (Figure S1). Detectable ABRs were elicited in Ush1c<sup>216AA</sup> mice that received local treatments of ASO-29, compared with little/no ABRs in untreated control mutant mice (Figures 3 and 4). Figure 3A illustrates representative recordings in response to 11.3-kHz pure tone exposure at 4 weeks of age from an untreated and treated Ush1c<sup>216AA</sup> mutant mouse injected with 30 µg of ASO-29 via the RWM at P1. A significant and robust decrease of 40–55 dB in ABR thresholds at low to middle frequencies (5.6–22.6 kHz) was observed in Ush1c<sup>216AA</sup> mice treated with ASO-29 by RWM injection at P1, compared with control mutant littermates ( $p < 0.001$ ) (Figure 3B). Most Ush1c<sup>216AA</sup> mice treated by RWM injection with ASO-29 (22/35; ~60%) recovered auditory sensitivity with thresholds below 60 dB with 8- to 16-kHz pure tone stimulation, 9 (~26%) of which had thresholds below 40 dB (Figures 3A and 3B). Although responses with RWM treatment

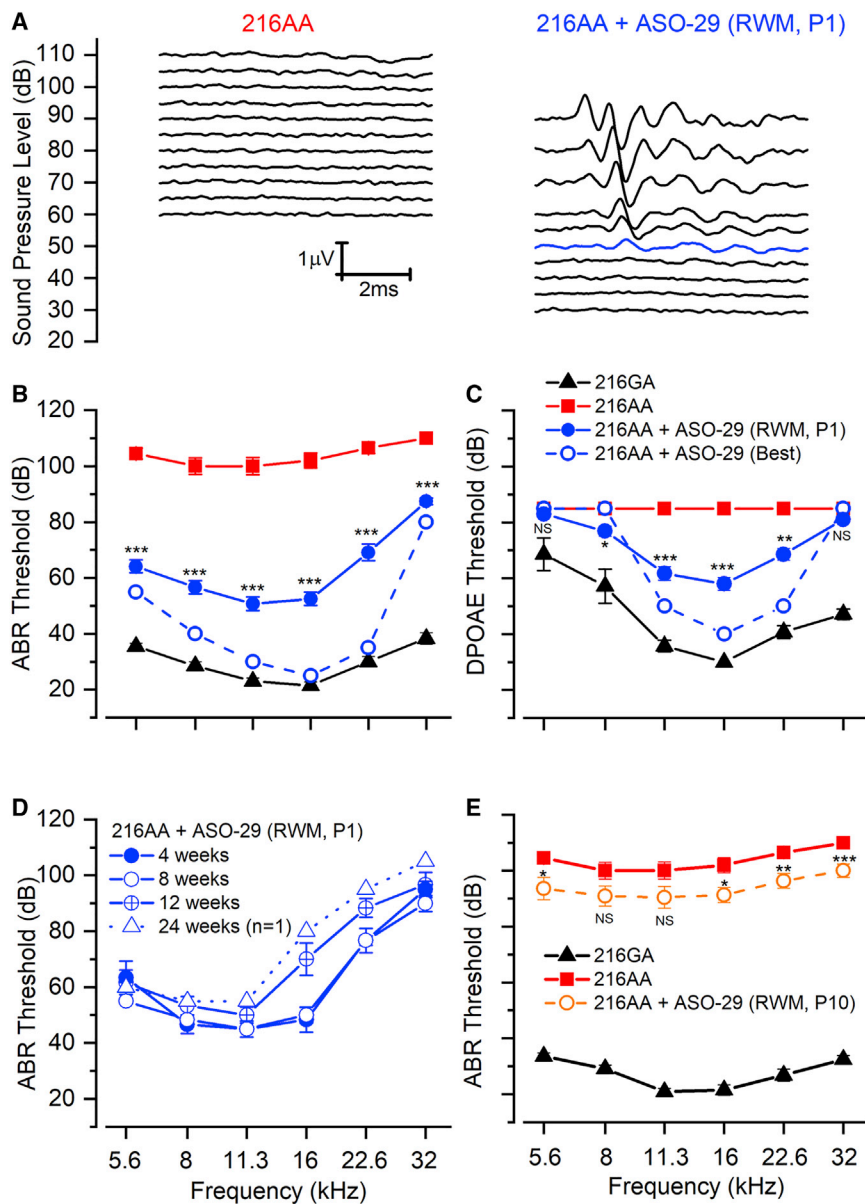


**Figure 3. RWM Injection of ASO-29 Improves Hearing in Ush1c<sup>216AA</sup> Mice**

ABRs and DPOAEs recorded from Ush1c<sup>216AA</sup> mice treated with 30 μg of ASO-29 (216AA+ASO-29) at P1 or P10 via RWM injection, and from untreated Ush1c mutant (216AA) and heterozygous (216GA) control littermates. (A) Representative ABR responses to pure tone stimulation at 11.3 kHz from 1-month-old 216AA+ASO-29 at P1 mice (right panel) and 216AA control mice (left panel). (B) Average ABR thresholds in 216AA+ASO-29 at P1 (blue filled circles, n = 35), 216AA+ASO-29 at P1 best performer (blue open circles, n = 1), and untreated 216AA (red filled squares, n = 10) and 216GA (black filled triangles, n = 10) control littermates. A significant reduction in the average ABR thresholds (blue line) was observed at all frequencies tested. (C) DPOAE thresholds in 216AA+ASO-29 at P1 via RWM (blue filled circles, n = 35), 216AA+ASO-29 at P1 best performer (blue open circles, n = 1), and untreated 216AA (red filled squares, n = 10) and 216GA (black filled triangles, n = 10) control littermates. A significant reduction in the average DPOAE thresholds (blue line) was observed to mid-frequencies stimulation (11.3–22.6 kHz). (D) ABR recovery as maintained for 24 weeks (n = 3 and 1, respectively). (E) RWM injections at P10 in 216AA mice (orange open circles, n = 10) did not rescue ABR thresholds. Data are represented as mean ± SEM. \*p ≤ 0.05, \*\*p ≤ 0.01, \*\*\*p ≤ 0.001 (one-way ANOVA). NS, not significant; RWM, round-window membrane; P, postnatal day.

were variable, the ASO-treated Ush1c<sup>216AA</sup> mouse with the best recovery had ABR responses close to those of normal hearing littermates (216GA) (Figure 3B). For all ASO-29-treated Ush1c<sup>216AA</sup> mice, recovery of ABRs was significant over the entire frequency range (p < 0.001), although it was less robust for higher frequencies, with best thresholds near 80 dB for exposure to 32-kHz pure tones. DPOAEs were also recovered demonstrating that ASO-29 injected through the RWM at P1 was able to rescue OHC function in Ush1c<sup>216AA</sup> mice. The best performer recovered nearly normal DPOAE thresholds in the mid-frequency range (11.3–22.6 kHz, Figure 3C). Rescued auditory thresholds at low frequencies (5.6–11.3 kHz) were maintained for up to 24 weeks (Figure 3D). At 12 weeks of age, a 10–20 dB loss of sensitivity was observed in the mid- to

high-frequency range (>16 kHz) (Figure 3D). RWM treatment of a lower dose of ASO-29 (3 μg) at P1 only slightly improved ABR thresholds in treated versus untreated Ush1c<sup>216AA</sup> mice: eight mice had ABR thresholds between 85 and 100 dB, and one had thresholds down to 65 dB (Figure S3). ABR thresholds of Ush1c<sup>216AA</sup> mutant mice did not improve when mice were treated with 30 μg of ASO-29 by RWM injection at P10 (Figure 3E). In addition, no ABR improvement was observed in Ush1c<sup>216AA</sup> mutant mice treated with

30 μg of ASO-29 fused to fluorescein by RWM injection at P1, suggesting that the fluorescein label interferes with ASO-29’s ability to target the 216A mutation (Figure S3), or with 30 μg of ASO-C via RWM injection at P1 (Figure S3). Treatment of heterozygous Ush1c<sup>216GA</sup> normal-hearing control mice with RWM injections of ASO-29 at P1, however, led to a small but significant increase in ABR thresholds up to 16 kHz (≤15-dB shift, p < 0.05), most likely due to the surgical procedure (Figure S3). These results demonstrate that RWM injection of ASO-29 in Ush1c<sup>216AA</sup> mice significantly improves hearing thresholds.

Next, we assessed hearing function in Ush1c<sup>216AA</sup> mice following local ASO treatment via the TM. ASO-29 was either applied

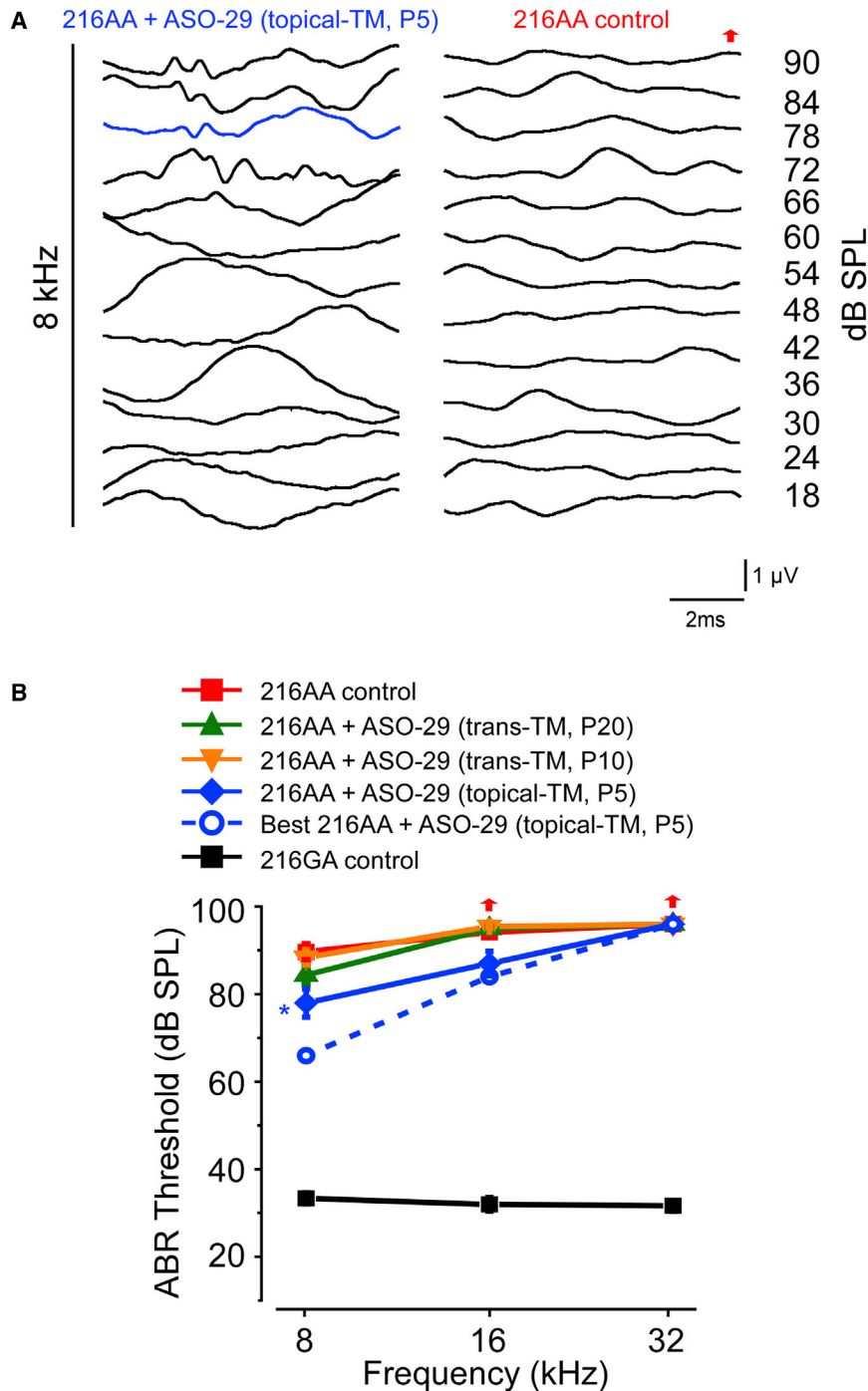


**Figure 4. TM Treatment with ASO-29 Improves Hearing in Ush1c<sup>216AA</sup> Mice**

ABRs were recorded from Ush1c<sup>216AA</sup> mice treated with 100–200 μg of ASO-29 (216AA+ASO-29) via topical-TM application with gel foam at P5, or by trans-TM injection at P10 or P20, and from Ush1c mutant (216AA) and heterozygous (216GA) and homozygous (216GG) control (saline, ASO-C/ASO-29 or untreated) littermates. (A) Representative ABR responses to pure tone stimulation at 8 kHz from 1-month-old 216AA+ASO-29 at P5 (topical-TM) and 216AA control mice. Thresholds are indicated by the colored line. (B) Average ABR thresholds in 216AA+ASO-29 at P5 (topical-TM, blue line, n = 8), 216AA+ASO-29 at P10 (trans-TM, orange line, n = 30), and 216AA+ASO-29 at P20 (trans-TM, green line, n = 17) and 216AA (ASO-C [n = 4], saline [n = 5], or untreated [n = 10], red line) and 216GA/GG (ASO-29 [n = 13], saline [n = 8/1], or untreated [n = 7/6], black line) control littermates. A moderate ~10 dB reduction in ABR thresholds was observed at 8 kHz in 216AA mice treated ASO-29 by topical-TM treatment at P5 (blue line). The best ASO-29-treated performer is represented (blue dotted line/open circles). Data are represented as mean ± SEM. \*p ≤ 0.05 (one-way ANOVA with Bonferroni post-test) indicates significant difference from control mutants (216AA). TM, tympanic membrane; P, postnatal day; SPL, sound pressure level.

topically to the TM (topical-TM) with gel foam at P5, or via trans-TM injection at P10 or P20. ABRs were detected in Ush1c<sup>216AA</sup> mice treated via TM application (topical-TM) of ASO-29; however, the signal-to-noise ratio of peaks 1–4 was low (Figure 4A). Remarkably, 1-month-old Ush1c<sup>216AA</sup> mice treated with 100 μg of ASO-29 by topical-TM placement at P5 had significantly reduced ABR thresholds in response to low-frequency (8-kHz) stimulation compared

moderately improves hearing thresholds in response to low-frequency stimulation.

#### Local Delivery of ASO-29 to the Middle and Inner Ear Improves Balance in Usher Mice

Systemic treatment of Ush1c<sup>216AA</sup> mice with ASO-29 within the first 2 weeks of life has been associated with recovery of balance function

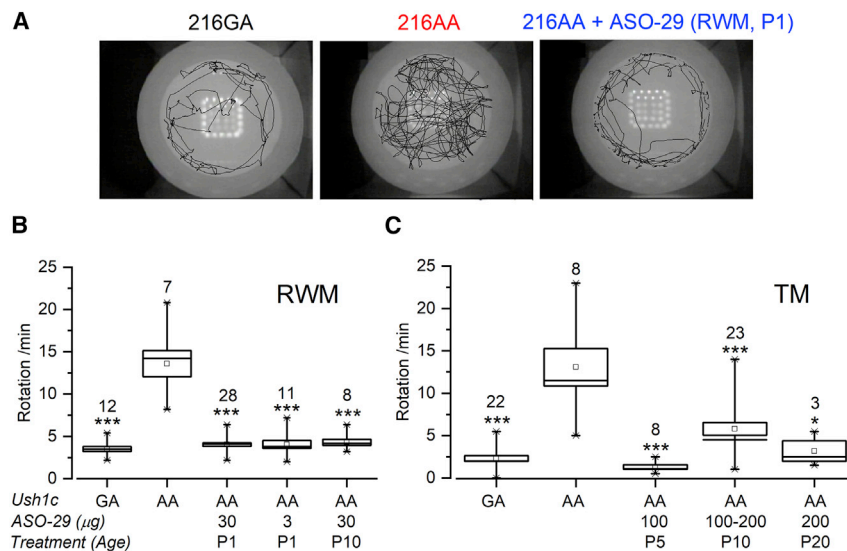


**Figure 5. Local Delivery of ASO-29 to the Ear Corrects Balance Behavior in *Ush1c*<sup>216AA</sup> Mice**

Open-field analysis of balance behavior in 1-month-old *Ush1c*<sup>216AA</sup> mice treated with various doses of ASO-29 at P1 or P10 via RWM injection, at P5 via topical-TM application with gel foam, or at P10 or P20 via trans-TM injection, as well as *Ush1c* mutant (216AA) and heterozygous (216GA) control (saline, ASO-C/ASO-29, or untreated) littermates. (A) Representative open-field images of the foot pattern in a 42cm wide arena of an *Ush1c*<sup>216AA</sup> mouse treated with ASO-29 via RWM injection at P1 (216AA+ASO-29, right panel), an untreated *Ush1c*<sup>216AA</sup> mouse (216AA, middle panel from<sup>21</sup>), and an *Ush1c*<sup>216GA</sup> mouse (216GA, left panel). (B and C) Quantitation of the number of rotations/min in (B) 216AA+ASO-29 at P1 (30, 3 μg) and P10 (30 μg) via RWM; (C) 216AA+ASO-29 at P5 via topical-TM (100 μg); 216AA+ASO-29 at P10 or P20 via trans-TM (100-200 μg); and 216AA and 216GA control littermates. Data are represented as mean ± SEM. \**p* ≤ 0.05, \*\**p* ≤ 0.01, \*\*\**p* ≤ 0.001 (one-way ANOVA with Tukey-Kramer post-test) indicate significant difference from control mutants (216AA). Number of mice assayed is indicated above boxes. RWM, round-window membrane; TM, tympanic membrane; P, postnatal.

and behavior.<sup>15-17</sup> To assess the effect of local ear ASO treatment on balance behavior, 1-month-old *Ush1c*<sup>216AA</sup> mice treated with ASO-29 via RWM at P1 (3 or 30 μg), P10 (30 μg), topical-TM at P5 (100 μg), or trans-TM injection at P10–P20 (100–200 μg) were observed in an open-field chamber and motion was analyzed to quantify the number of rotations per minute. *Ush1c*<sup>216AA</sup> mice exhibit circling behavior indicative of a vestibular deficit<sup>14</sup> (Figure 5A). Impressively, treatment of *Ush1c*<sup>216AA</sup> mice with ASO-29 via the RWM or TM at all ages and doses tested significantly reduced circling behavior (*p* ≤ 0.05, Figures 5B and 5C). Moreover, we did not observe a return of circling behavior in *Ush1c*<sup>216AA</sup> mice treated with ASO-29 via RWM or TM at all ages after 2 years, suggesting a long duration of treatment effect. These results demonstrate that ASO-29 delivered to the inner or middle ear prior to P20 significantly improves balance behavior.

To further assess vestibular functional recovery after inner ear injection, mice injected at P1 were assessed for rotational vestibulo-ocular reflex (RVOR) tests. For this latest experiment, ASOs were injected directly into the endolymph using a method similar to the semi-circular canal injection with the injection pipette placed closer to the utricle. While similar transfection rates were obtained in a previous study using RWM and endolymph injection of AAV, the later method was more reliable and thereby adopted for the tail end of this study<sup>26</sup>. Quantitative analysis revealed variable but significant recovery of the rotational VORs in ASO-29-treated *Ush1c*<sup>216AA</sup> mice (*p* < 0.001; Figures 6A and 6B). While untreated *Ush1c*<sup>216AA</sup> mice had no VORs, all *Ush1c*<sup>216AA</sup> mice treated with ASO-29 had detectable responses with average gains between 0.44 and 0.6, with best performers similar to WT levels (Figure 6A). In the absence of VORs, no phase could be determined in *Ush1c*<sup>216AA</sup> untreated control mice, while ASO-29-treated *Ush1c*<sup>216AA</sup> mice exhibited comparable VOR phases to those of WT mice (Figure 6B).

To better gauge the extent of vestibular peripheral recovery, single-unit recordings of vestibular afferents were performed *in vivo*. A total of 281 afferents were recorded from the vestibular nerve bundles of three WT mice (*n* = 113), three ASO-29-treated mice, and three untreated *Ush1c*<sup>216AA</sup> mice (*n* = 120 and *n* = 48 afferents, respectively). Figures 7A–7C show examples of vestibular afferent responses to head rotation recorded from a WT, untreated, and ASO-29-treated *Ush1c*<sup>216AA</sup> mouse. Afferents recorded from the untreated *Ush1c*<sup>216AA</sup> mouse exhibited significantly lower spontaneous firing rates than those from the WT mice. ASO-29 treatment significantly restored the spontaneous firing rate of both regular and irregular afferents (Figure 7D, one-way ANOVA and *post hoc* Holm-Sidak tests, *p* < 0.01). The percentage of afferents responsive to head rotation was 49.6%, 27.5%, and 16.7% for WT, ASO-29-treated, and untreated *Ush1c*<sup>216AA</sup> mice, respectively. ASO-29 treatment partially restored the irregular, but not regular, afferent sensitivity to head rotation (Figure 7E, *t* test, one-tailed, *p* = 0.0145). Afferents recorded from the untreated *Ush1c*<sup>216AA</sup> mouse were less irregular than those from the WT mice (Figure 7F). ASO-29 treatment in *Ush1c*<sup>216AA</sup> mice significantly increased irregularity of vestibular afferents, to levels similar to the WT mice (one-way ANOVA and *post hoc* Holm-Sidak tests, *p* = 0.003). These results demonstrate that inner ear treatment of *Ush1c*<sup>216AA</sup> mice with ASO-29 restores the afferent baseline firing rate, sensitivity to head rotation, and irregularity of vestibular afferents.

#### Local Delivery of ASO-29 to the Middle and Inner Ear Corrects *Ush1c* Pre-mRNA Splicing and Restores Harmonin Expression in the Cochlea of *Ush1c*<sup>216AA</sup> Mice

Systemic injections of ASO-29 in neonatal *Ush1c*<sup>216AA</sup> mice have been shown to improve correct splicing of the *Ush1c* gene, restore harmonin expression and hair bundle morphology, and promote

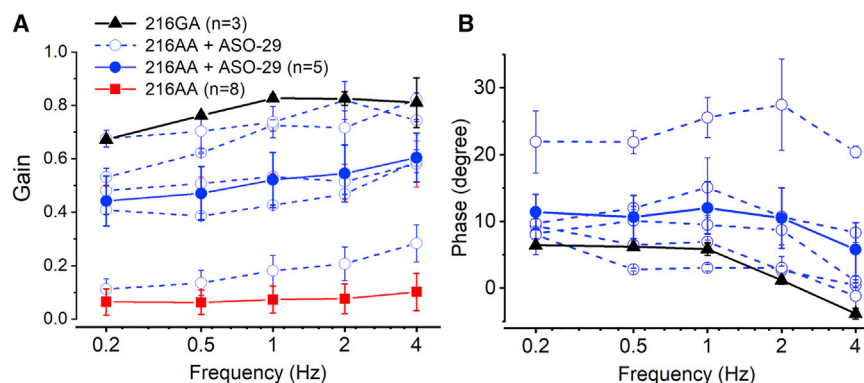


**Figure 6. Local ASO-29 Treatment Restores Rotational VOR in *Ush1c*<sup>216AA</sup> Mice**

(A and B) Gains (A) and phases (B) of rotational vestibulo-ocular reflex (VOR) responses of untreated (red) and ASO-29-treated *Ush1c*<sup>216AA</sup> (blue) mice, and wild-type (WT) (black) mice. Solid lines indicate group averages; dotted lines indicate an individual 216AA+ASO-29-treated mouse. Data are represented as mean  $\pm$  SEM. Pairwise multiple comparison procedures (Holm-Sidak method) show that ASO-29 treatment significantly improves VOR gain ( $p < 0.001$ ) for all frequencies tested and leads to significant recovery of the VOR phase near the WT level ( $p < 0.001$ ).

hair cell survival in the ear.<sup>15–17</sup> First, we assessed whether local injections of ASO-29 improved *Ush1c* splicing and harmonin expression in the inner ear. Full-length *Ush1c* mRNA produced by correct splicing was detected in *Ush1c*<sup>216AA</sup> mice treated with ASO-29 via RWM at P1, via topical-TM application at P5, and via trans-TM injection at P20 (Figure 8A). The highest levels of correct *Ush1c* splicing were observed after RWM injections at P1, with the next most efficient strategy from topical-TM application at P5 (Figure 8B). Treatments at P10 by trans-TM injection showed little improvement in *Ush1c* splicing (Figures 8A and 8B).

To assess whether splicing correction with local ear ASO-29 treatment was associated with recovery of harmonin expression and localization in hair cell bundles, we performed harmonin-b immunostaining of cochleae prepared from *Ush1c*<sup>216AA</sup> mice treated with ASO-29 via RWM at P1 or by topical-TM application at P5, and control littermates. Increased harmonin-b fluorescent labeling was observed at the tips of the stereocilia bundle after both RWM and topical-TM delivery of ASO-29, demonstrating the recovery of harmonin expression at the tip of the stereocilia (Figure 8C). These data show that ASO-29 delivered directly to the inner and middle ear improves *Ush1c* splicing and harmonin expression in the ear.

#### Local Delivery of ASO-29 to the Inner Ear Improves Hair Cell Bundle Morphology and Survival in the Cochlea of *Ush1c*<sup>216AA</sup> Mice

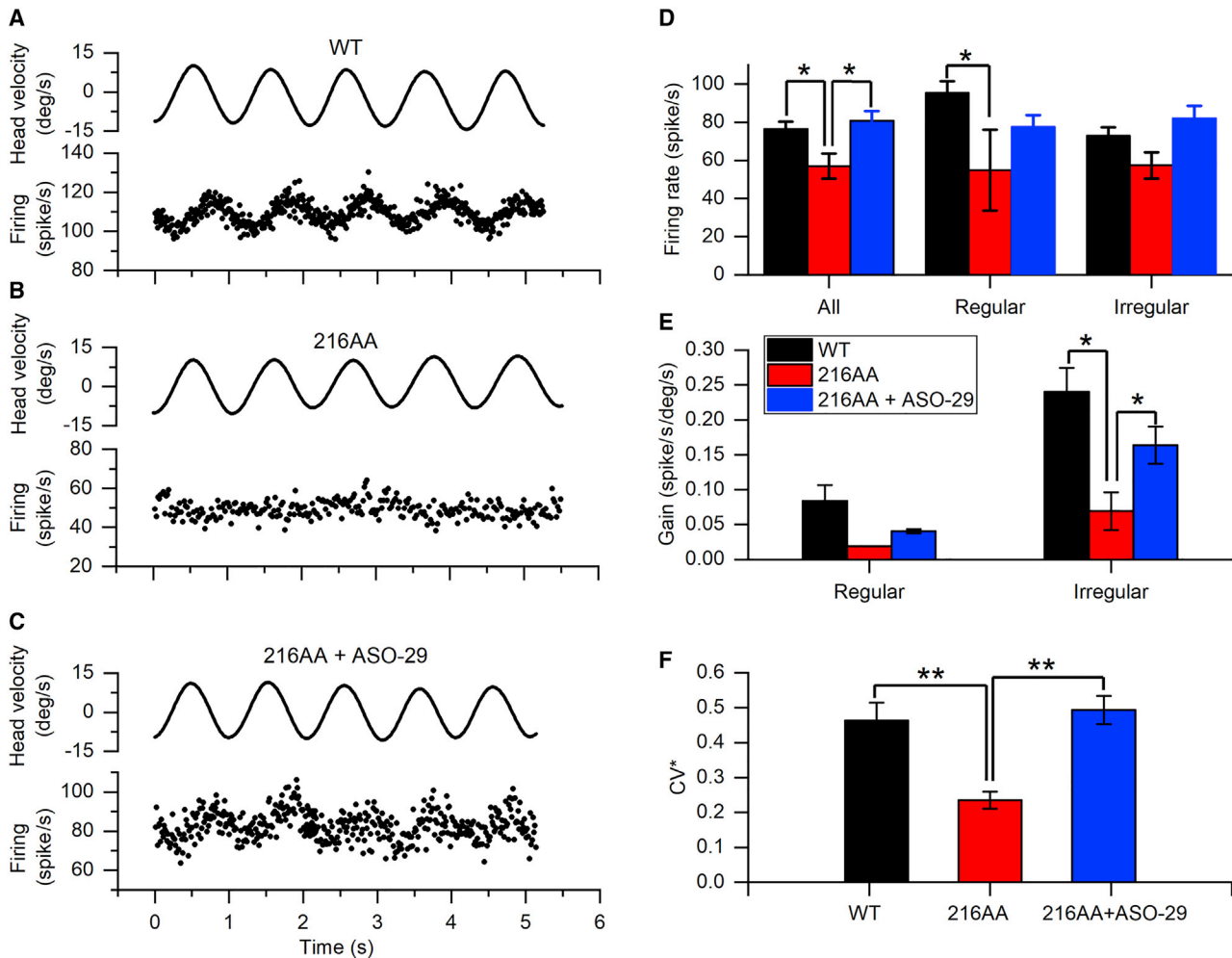
*Ush1c*<sup>216AA</sup> mice have severely abnormal hair cell bundle morphology and significantly fewer auditory hair cells by 1 month of age.<sup>14</sup> Systemic injections of ASO-29 in neonatal *Ush1c*<sup>216AA</sup> mice are associated with improved hair cell bundle morphology and survival.<sup>15</sup> To assess whether local delivery of ASO-29 could improve hair cell structures, we performed scanning electron microscopy (EM) on the cochleae from *Ush1c*<sup>216AA</sup> mice at 4 weeks of age that were treated with ASO-29 via RWM injection at P1, and control littermates (Figure 8D). OHC bundles, while not the typical V- or W-shape of normal hearing WT littermates, had significantly improved morphology in all regions of the cochlea (apex, middle-turn, and base) compared with untreated control mutants. Additionally, *Ush1c*<sup>216AA</sup> mice treated with ASO-29 by RWM injection at P1 had

increased numbers of OHCs in all regions of the cochlea. These results demonstrate that RWM injection at P1 of ASO-29 in *Ush1c*<sup>216AA</sup> mice improved OHC bundle morphology and cell survival.

#### DISCUSSION

In this study, we identified three new delivery routes using ASOs for the efficacious treatment of hearing and balance deficits in a mouse model of human Usher syndrome. Previous work has demonstrated that systemic treatment of *Ush1c* c.216G>A (*Ush1c*<sup>216AA</sup>) mice with ASOs designed to target the 216A mutation (ASO-29) restores gene and protein expression in the ear, and leads to partial recovery of auditory and balance function.<sup>15–17</sup> Herein, we demonstrate that localized delivery of ASO-29 directly to either the inner or the middle ear of *Ush1c*<sup>216AA</sup> mice improves hearing thresholds and balance behavior. Our results show that RWM injection of ASO-29 at P1 in *Ush1c*<sup>216AA</sup> mice robustly restores low- to mid-frequency hearing thresholds, similar to systemic treatment. Remarkably, a less invasive treatment in young mice using ASO-29 with gel foam applied topically to the developing TM through the external auditory canal (EAC), while less robust than surgical RWM or systemic injections (~12-dB shift compared with a 50- to 60-dB shift, respectively), led to significant recovery of the hearing threshold at a low frequency. All three local delivery routes tested, i.e., RWM injection, topical-TM application, and trans-TM injection, of ASO-29 treatment in *Ush1c*<sup>216AA</sup> mice showed significant improvements in balance behavior as assessed by observations in the open field. Additionally, ASOs injected directly into the inner ear led to significant recovery of VORs and vestibular afferent firing. Importantly, we demonstrate, for the first time, that ASOs delivered locally to the inner ear can successfully reach sensory hair cells and correct *Ush1c* 216A splicing. More significantly, this treatment led to an increase in harmonin expression at the tips of the stereocilia hair cell bundle, improvements in hair cell bundle morphology and survival, and recovery of mechanotransduction. Our results support the delivery of ASOs directly to the inner and middle ear for the treatment of hearing and balance disorders associated with Usher syndrome.

The success rate of treatment in *Ush1c*<sup>216AA</sup> mice, defined as rescued ABR thresholds at 60 dB or lower in response to stimulation at 8 kHz,

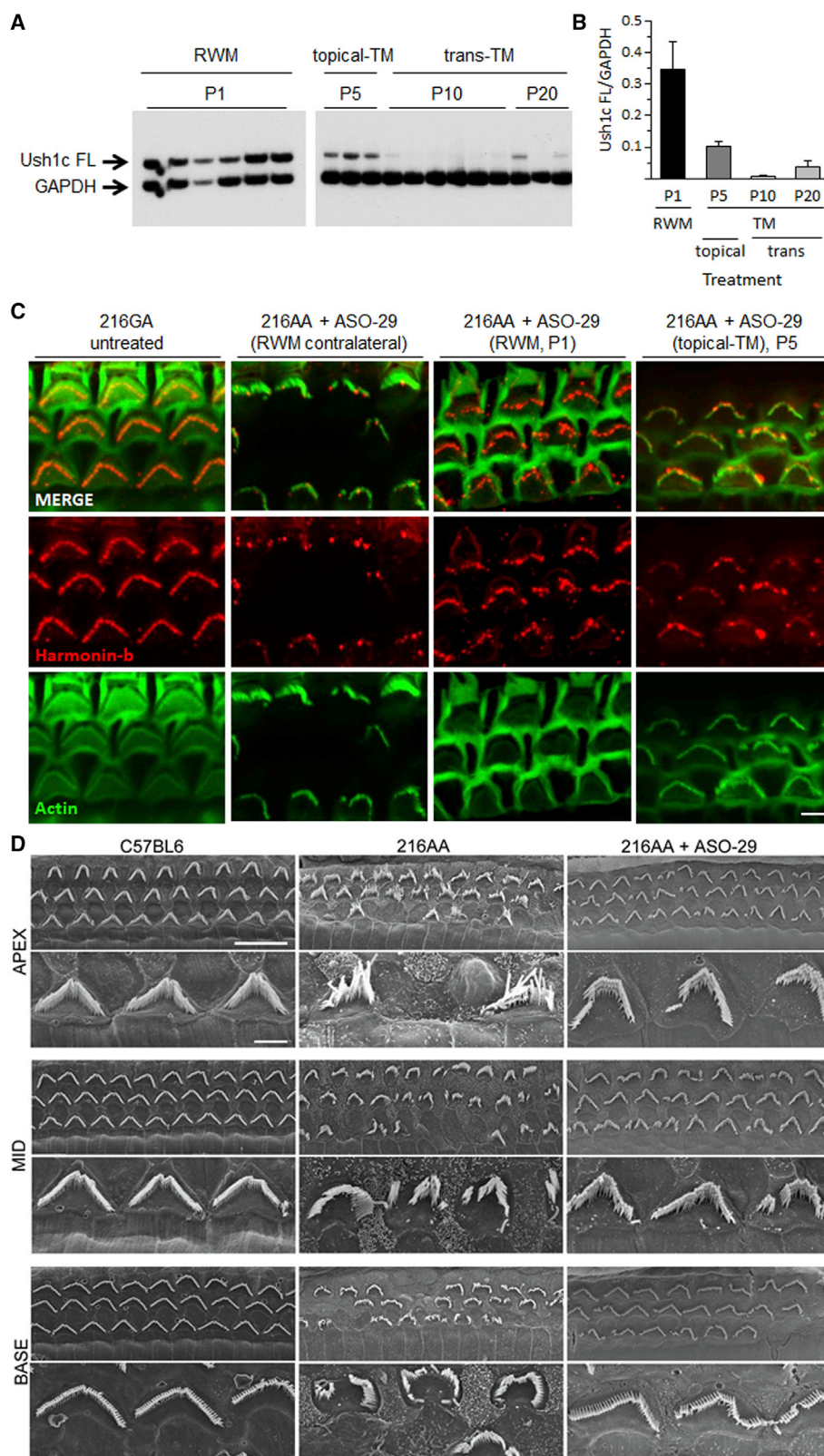


(A–C) Representative responses of vestibular afferents recorded from WT (A), untreated- (B) and ASO-29-treated-Ush1c<sup>216AA</sup> mice during 1-Hz earth-horizontal rotation. Top traces indicate head velocity; bottom traces indicate discharge activity of the afferent. (D) Average baseline firing rates of WT (n = 113 afferents total from three mice), ASO-29-treated- (n = 120 afferents total from three mice) and untreated-Ush1c<sup>216AA</sup> mice (n = 48 afferents total from three mice). (E) Average gains to head rotation of WT, ASO-29-treated- and untreated-Ush1c<sup>216AA</sup> mice. (F) Regularity of WT, ASO-29-treated- and untreated-Ush1c<sup>216AA</sup> mice. deg, degrees; CV\*, coefficient of variation of interspike intervals. Data are represented as mean ± SEM. \*p ≤ 0.05, \*\*p ≤ 0.01, (one-way ANOVA).

was surprisingly very similar for RWM treatment at P1 with either ASO treatment or gene replacement with AAV<sup>21</sup> (at about 77%), both of which were slightly lower than systemic delivery at the same age (88%)<sup>16</sup> (J.J.L., unpublished data). The failed rescues are likely the results of unsuccessful injections. All data were included in our analysis, regardless of the outcome. For those with successful recovery, the average improvement in hearing thresholds was comparable in 1-month-old Ush1c<sup>216AA</sup> mice after RWM or systemic injection at P1 of ASO-29 or AAV-expressing harmonin b.<sup>15,21</sup> Moreover, ABR thresholds in ASO-29- or AAV-treated Ush1c<sup>216AA</sup> mice remained stable for 3 months after a single treatment at P1. Indeed, while long-term maintenance of the recovery was observed, a decline in mid- to high-frequency thresholds is evident by 6 months of age for local RWM delivery and also i.p. injections of ASO-29 (the present

study and Lentz et al.<sup>15</sup>). While multiple dosing may be required to achieve sustained hearing rescue, our results suggest that delivery to the middle ear, for example via trans-tympanic injection, may be an efficacious re-dosing strategy.

Interestingly, while RWM treatment with a low dose of ASO-29 at P1 or treating later, at P10, failed to recover auditory sensitivity (Figure 3E; Figure S3), a similar and significant reduction of the circling behavior was observed in the two cohorts (p < 0.001; Figure 5B). Furthermore, P10 and P20 trans-TM treatments also led to significant reduction of circling behavior, demonstrating that ASO-29 was able to reach inner ear vestibular tissues after delivery to the middle ear. Why the vestibular system is more amenable to treatment over a longer time window is unclear. Vestibular hair cells are perhaps not



(legend on next page)

as susceptible to the disruption in harmonin expression. Indeed, no vestibular hair cell loss was observed by 1 month of age in utricles (Figure S2), in contrast with significant loss of auditory hair cells at the same age<sup>15,21</sup> (Figures 8C and 8D). With about 50% of vestibular hair cells added after birth, mostly during the first postnatal week,<sup>27,28</sup> the vestibular system is still largely immature at birth. Additionally, postnatal expression of *Ush1c* peaks at P16 in vestibular hair cells of the utricle, while the peak in cochlear hair cells is P7 (SHIELD Harvard Inner-Ear Laboratory Database, <https://shield.hms.harvard.edu/index.html>). The delayed development and maturation and *Ush1c* expression in the vestibular system may extend the window of opportunity for therapeutic intervention. Finally, while limited, regeneration of vestibular hair cells does occur in younger animals and can be promoted after damage, which may facilitate therapeutic recovery at later time points.<sup>29–31</sup> Taken together, these results suggest that vestibular hair cells are amenable to treatments at later stages.

ASO-29 treatment *in utero* has been shown to be well tolerated and lead to recovery of auditory and vestibular function that correlates with the correction of gene and protein expression in postnatal *Ush1c*<sup>216AA</sup> mice.<sup>32,33</sup> Delivery of ASO-29 via intra-otic injection on embryonic day 12.5 in *Ush1c*<sup>216AA</sup> mice, equivalent to gestational week 12 in human development, demonstrates the feasibility of preventing the disease phenotype. The advantage of an early intervention is that it may allow access to developing embryonic tissue at a time critical for the generation of the sensory hair cells of the inner ear. Early treatment becomes important when considering therapies that target genes involved in hair cell formation and maturation, particularly those that develop first in the basal region of the auditory organ. Indeed, both our study and those by Lentz et al.<sup>15</sup> and Ponnath et al.<sup>16</sup> show that recovery in the high-frequency region is not complete. Similar observations were made when using AAV vectors expressing correct harmonin.<sup>21</sup>

Variability in efficacy and side effects in treating humans with hearing and balance disorders has led to advances in inner ear drug delivery.<sup>34</sup> Following local delivery in humans and animals, the distribution of drugs, including corticosteroids, antibiotics, antioxidants, and gene-based therapies, occurs by passive diffusion in the cochlea<sup>35–38</sup> with a base-to-apex concentration gradient. In this study, we observed that ASO-29 reached hair cells throughout the cochlea, but most robustly only rescued hearing at low and mid frequencies, which are important for human speech.<sup>39</sup> The pharmacokinetics of ASO-

29 distribution and clearance in the cochlea are needed to better understand its mechanism of action in the inner ear.

Our results further support the use of ASOs therapeutically for mRNA splicing correction and demonstrate that local applications lead to improved outcomes. While similar ABR thresholds have been observed after treatments with AAV driving expression of WT harmonin,<sup>21</sup> ASO treatments offer two advantages. First, ASOs do not alter endogenous expression levels but rather correct gene expression at the mRNA level. This mechanism of action may be important for genes that express multiple isoforms that are temporally- and tissue-specific, such as those associated with Usher syndrome. Second, while 2'-O-methoxyethyl (2'-MOE) ASOs have been shown in limited studies to activate the innate immune response when delivered systemically long-term on a weekly basis,<sup>40,41</sup> they do not elicit an adaptive immune response and thus can be repeatedly dosed, unlike AAV therapeutics.<sup>42,43</sup> In this study, we observed that mice, including both heterozygous *Ush1c*<sup>216GA</sup> and homozygous *Ush1c*<sup>216AA</sup> mutants, treated with ASO-29 via the middle ear showed a wavy ABR pattern (Figures S4C and S4D). In contrast, mice treated with saline, or via systemic or inner ear injections, did not show this pattern (Figures S4A, S4B, and S4E). The cause of this abnormal ABR pattern following middle ear delivery of ASO-29 is not known; however, in WT mice treated with ASO-29, there was no change in ABR threshold for low- to mid-frequency kHz stimuli for all middle ear deliveries or wave I latency (Figure S5) that is typically associated with middle ear fluid or inflammation.<sup>44–47</sup>

Currently, there are numerous oligonucleotide drugs carrying the 2'-MOE modification that are commercially available for use in humans or in clinical trials. An ASO therapy is now being considered for the treatment of vision loss associated with Usher syndrome type 2A (ClinicalTrials.gov: NCT03780257; PQ-421a-001, phase 1/2 clinical trial, ProQR, targets USH2A). Our work and the work of others demonstrate that ASO treatment can successfully restore hair cell function. Development of larger animal models for inherited deafness, including Usher syndrome, will be important to determine the safety and feasibility of such therapies to restore hearing.

We demonstrate that local delivery of ASO-29 rescues hearing and balance in *Ush1c* c.216G>A knockin mice and provide proof in principle of successful implementation of local delivery of small molecule therapy for hearing and balance disorders.

### Figure 8. Local Delivery of ASO-29 to the Ear Corrects *Ush1c* Splicing, Harmonin Protein Expression, and Hair Bundle Morphology in *Ush1c*<sup>216AA</sup> Mice

*Ush1c* mRNA and harmonin protein expression analysis in 1-month-old *Ush1c*<sup>216AA</sup> mice treated with ASO-29 via RWM injection at P1 (30 μg), topical-TM application at P5 (100–200 μg), or trans-TM injection at P10 or P20 (100–200 μg). (A) Full-length (FL) *Ush1c* and GAPDH RT-PCR products amplified from cDNA isolated from the cochleae of *Ush1c*<sup>216AA</sup> mice treated with ASO-29 through the RWM or TM. Data are represented as mean ± SEM. (B) Quantitation of RT-PCR products in (A). (C) Immunohistochemistry analysis of the cochlear middle-turn (1.8–2.2 mm from the apex tip) shows increased expression and localization of harmonin-b (red) at the tips of OHC stereocilia bundles (actin, green) in the treated ear of *Ush1c*<sup>216AA</sup> mice that received ASO-29 via RWM injection or topical-TM application, compared with the contralateral ear from a treated mouse. (D) Representative scanning electron micrographs show improved OHC bundle morphology and an increased number of OHC at the apex (left panel), middle-turn (Mid, center panel), and base (right panel) of the cochlea in *Ush1c*<sup>216AA</sup> mice (216AA) treated with 30 μg of ASO-29 via RWM injection at P1 (bottom row), compared with the abnormal bundle morphology and missing bundles in untreated *Ush1c*<sup>216AA</sup> control (middle row) mice. Scale bars indicate 10 μm. RWM, round-window membrane; TM, tympanic membrane; P, postnatal; FL, full length.

## MATERIALS AND METHODS

### Mice

*Ush1c* c.216G >A knockin mice on a C57BL6;129S6 background, negative for age-related hearing loss loci 1 (*ahli* [Cdh23<sup>753G</sup>]), were used for this study. All procedures used for this work met the NIH *Guidelines for the Care and Use of Laboratory Animals* and were approved by the Institutional Animal Care and Use Committees at Boston Children's Hospital (BCH; protocols 18-01-3610R, 17-03-3396R, and 15-01-2878R), Louisiana State University Health Sciences Center (LSUHSC; protocol 3541), and the University of Mississippi Medical Center (UMMC; protocol 1565). Mice were genotyped for *Ush1c* c.216G>A alleles from DNA isolated from a toe clip (before P8) and ear punch or tail snip (after P8) as described previously.<sup>13</sup> For all studies, both male and female mice were used in approximately equal proportions.

### Oligonucleotides

ASOs were synthesized as previously described.<sup>1</sup> ASO-C (5'-TTAGTTTAATCACGCTCG-3') and ASO-29 (5'-AGCTGATCA TATTCTACC-3'), previously validated, have a fully modified phosphorothioate backbone with 2'-MOE modifications. The dosing solution was prepared in sterile hood from a stock solution diluted with sterile saline. For RWM and utricle injections, ASOs were prepared at 3 and 30  $\mu\text{g}/\mu\text{L}$ . For TM treatments, ASOs were prepared at 100–200  $\mu\text{g}/\mu\text{L}$ .

### Tissue Preparation for Single-Cell Electrophysiological

#### Recordings

Cochlear organs of Corti were harvested on P6 from ASO-treated (RWM injection on P1) or untreated *Ush1c* c.216G>A heterozygous (*Ush1c*<sup>216GA</sup>) or homozygous (*Ush1c*<sup>216AA</sup>) mutant mice and maintained in culture for electrophysiological studies. Cultures were maintained for 9–10 days with 1% fetal bovine serum. Electrophysiological recordings were performed in standard artificial perilymph solution containing 144 mM NaCl, 0.7 mM NaH<sub>2</sub>PO<sub>4</sub>, 5.8 mM KCl, 1.3 mM CaCl<sub>2</sub>, 0.9 mM MgCl<sub>2</sub>, 5.6 mM D-glucose, and 10 mM HEPES-NaOH, adjusted to pH 7.4 and 320 mOsmol/kg. Vitamins (1:50) and amino acids (1:100) were added from concentrates (Invitrogen, Carlsbad, CA, USA). Hair cells were viewed from the apical surface using an upright Axioskop FS microscope (Zeiss, Oberkochen, Germany) equipped with a  $\times 63$  water immersion objective with differential interference contrast optics. Recording pipettes (3–5 macrophages) were pulled from borosilicate capillary glass (Garner Glass, Claremont, CA, USA) and filled with intracellular solution containing 135 mM KCl, 5 mM EGTA-KOH, 10 mM HEPES, 2.5 mM K<sub>2</sub>ATP, 3.5 mM MgCl<sub>2</sub>, and 0.1 mM CaCl<sub>2</sub> (pH 7.4). Currents were recorded under whole-cell voltage clamp at a holding potential of  $-64$  mV at room temperature. Data were acquired using an Axopatch multiclamp 700A or Axopatch 200A (Molecular Devices, Palo Alto, CA, USA) filtered at 10 kHz with a low-pass Bessel filter, digitized at  $\geq 20$  kHz with a 12-bit acquisition board (Digidata 1322) and pClamp 8.2 and 10.5 (Molecular Devices, Palo Alto, CA, USA). Data were analyzed offline with Origin 6.1 software (Origin-

Lab) and are presented as means  $\pm$  standard deviations (SDs) unless otherwise noted.

### Mechanical Stimulation of Hair Cell Bundles

Mechanical stimuli were transmitted via a stiff glass probe mounted on a one-dimensional PICMA chip piezo actuator (Physik Instruments, Waldbronn, Germany) driven by a 400-mA ENV400 amplifier (Piezosystem, Jena, Germany). The tip of the probe was fire polished (fire polisher, H602, World Precision Instruments, Sarasota, FL, USA) to fit the stereociliary bundle. Deflections were evoked by applying voltage steps filtered with an 8-pole Bessel filter (Khron-Hite, Brockton, MA, USA) at 50 kHz to eliminate residual pipette resonance. Hair bundle deflections were monitored using a C2400 charge-coupled device (CCD) camera (Hamamatsu, Japan). Voltage steps were used to calibrate the motion of the stimulus probe around  $\pm 2$   $\mu\text{m}$  of its rest position. Video images of the probe were recorded to confirm absence of off-axis motion and calibrate the probe motion (spatial resolution of  $\sim 4$  nm). The 10%–90% rise-time of the probe was  $\sim 20$   $\mu\text{s}$ .

### RWM and Utricle Injections of ASO-29

RWM and utricle injections were performed at BCH. 1- $\mu\text{L}$  ASO-29 preparations (3–30  $\mu\text{g}/\mu\text{L}$ ) were injected into one ear in neonatal mice at P0–P1 (P1) or P10–P12 (P10). P1 mice were anesthetized using hypothermia exposure. P10 mice were anesthetized with isoflurane. Upon anesthesia, a post-auricular incision was made to expose the otic bulla and visualize the cochlea. The utricle and RWM were identified visually with the aid of a stereomicroscope (Zeiss Stemi 2000). Injections were done through the RWM or the utricle with a glass micropipette controlled by a micromanipulator.<sup>48</sup> The rate of injection was controlled at approximately 0.02  $\mu\text{L}/\text{min}$  for 10 min. Standard post-operative care was applied.

### Topical-TM application of ASO-29

Topical-TM treatments were conducted at LSUHSC. 0.5  $\mu\text{L}$  of ASO-29 (100–200  $\mu\text{g}$ ) was delivered to one ear via topical-TM application at P5. Mice were anesthetized using hypothermia exposure. Following anesthesia, the EAC skin was separated with a microforceps, and a 1-mm round punch of gel foam was placed into the blind pouch of the medial EAC. For this procedure, a Hamilton syringe with a 33G needle was used to facilitate its insertion medially into the EAC and inject ASO-29 into the gel foam followed by re-approximation of the external meatus to its original adherent position.

### Trans-TM Injection of ASO

Trans-TM injections were conducted at LSUHSC. 0.5  $\mu\text{L}$  of ASO-29 (100–200  $\mu\text{g}$ ) or vehicle (saline) was injected into one ear through the TM in mice at P10–P11 (P10) or P20. Mice were anesthetized (ketamine/xylazine, 100/10 mg/kg, respectively, i.p.) and body temperature was maintained near 38°C with a heating pad. At P10, adherent fragile ear canal skin was carefully teased apart to expose the eardrum for injection with a 33G Hamilton syringe. Microforceps were used to retract the skin and visualize the medial superior fold adjacent to the tympanic membrane. A Hamilton syringe with 33G needle was used

to inject ASO-29 trans-tympanically. Postoperatively, pups were placed on a warmer in right lateral decubitus position until anesthesia wore off.

### Scanning EM

Scanning EM was performed at 4 weeks of age along the organ of Corti of Ush1c<sup>216GA</sup>, Ush1c<sup>216AA</sup>, and Ush1c<sup>216AA</sup> ASO-29-treated mice. Organ of Corti explants were fixed in 2.5% glutaraldehyde in 0.1 M cacodylate buffer (Electron Microscopy Sciences) supplemented with 2 mM CaCl<sub>2</sub> for 1 h at room temperature. Specimens were dehydrated in a graded series of acetone, critical-point dried from liquid CO<sub>2</sub>, sputter-coated with 4–5 nm of platinum (Q150T, Quorum Technologies, UK), and observed with a field emission scanning electron microscope (S-4800, Hitachi, Japan).

### RNA Isolation and RT-PCR

Cochlear tissue for RNA isolation was rapidly dissected following euthanasia and snap-frozen in liquid nitrogen. Tissue was stored at –80°C until shipment on dry ice. Frozen tissues were homogenized in TRIzol solution (Thermo Fisher Scientific) using a PowerGen 1000 homogenizer (Thermo Fisher Scientific). Total RNA was purified from TRIzol reagent following the manufacturer's recommendations. RNA was quantitated and purity assessed (A260/A280) using a BioPhotometer (Eppendorf). RNA (1 µg) was reverse transcribed using oligo(dT) primer and GoScript reverse transcriptase (Promega) following the manufacturer's recommendations. Semiquantitative PCR was performed using 1 µL of cDNA and GoTaq Green (Promega) supplemented with primers and  $\alpha$ -<sup>32</sup>P-deoxycytidine triphosphate (dCTP). Primers specific for human *USH1C* exon 3 (5'-GAA TATGATCAGCTGACC-3') and mouse exon 5 (5'-TCTCACTTT GATGGACACGGTCTTC-3') were used to specifically amplify only mRNA generated from the knocked-in allele of the human *USH1C* c.216A gene, which is only present in correctly spliced mRNA. Mouse *Gapdh* primers (5'-GTGAGGCCGGTGCTGAG TATG-3' and 5'-GCCAAAGTTGTCATGGATGAC-3') were used to detect and measure endogenous murine *Gapdh* mRNA. Products were separated on a 6% non-denaturing polyacrylamide gel and quantitated using a Typhoon 9400 phosphorimager (GE Healthcare).

### ABRs and DPOAEs: BCH Location

Hearing function was assessed at BCH as described by Pan et al.<sup>21</sup> Briefly, ABRs and DPOAEs were recorded from mice anesthetized with xylazine (5–10 mg/kg, i.p.) and ketamine (60–100 mg/kg, i.p.). Subcutaneous needle electrodes were inserted into the skin (1) dorsally between the two ears (reference electrode), (2) behind the left pinna (recording electrode), and (3) dorsally at the rump of the animal (ground electrode). The meatus at the base of the pinna was trimmed away to expose the ear canal. For ABR recordings the ear canal and hearing apparatus (EPL acoustic system, MEEI, Boston, MA, USA) were presented with 5-ms tone pips. The responses were amplified (10,000 times), filtered (0.1–3 kHz), and averaged with an analog-digital board in a PC based data-acquisition system (EPL cochlear function test suite, MEEI, Boston, MA, USA). Sound level was raised

in 5- to 10-dB steps from 0- to 110-dB sound pressure level (SPL) and frequencies between 5.2 and 32 kHz. At each level, 512–1,024 responses were averaged (with stimulus polarity alternated) after “artifact rejection.” Thresholds were determined using a peak discriminator algorithm (ABR Peak Analysis software, v1.5.7.60, EPL) and by visual inspection. Data were analyzed and plotted using Origin 2015 (OriginLab, MA, USA). Thresholds averages  $\pm$  SDs are presented unless otherwise stated. For DPOAEs, f1 and f2 primary tones (f2/f1 = 1.2) were presented with f2 varied between 5.6 and 45.2 kHz in half-octave steps and L1–L2 = 10-dB SPL. At each f2, L2 was varied between 10- and 80-dB SPL in 10-dB SPL increments. DPOAE threshold was defined from the average spectra as the L2 level eliciting a DPOAE of magnitude 5-dB SPL above the noise floor. The mean noise floor level was under 0-dB SPL across all frequencies. Stimuli were generated with 24-bit digital I-O cards (National Instruments PXI-4461) in a PXI-1042Q chassis, amplified by an SA-1 speaker driver (Tucker-Davis Technologies) and delivered from two electrostatic drivers (CUI CDMG15008-03A) in our custom acoustic system. An electret microphone (Knowles FG-23329-P07) at the end of a small probe tube was used to monitor ear-canal sound pressure. Most of these experiments were not performed under blinded conditions.

### ABRs: LSUHSC Location

Hearing threshold was assessed by ABR analysis as described by Pon-nath et al.<sup>16</sup> Briefly, ABRs were recorded in Ush1c<sup>216AA</sup> mutant mice treated with ASO-29 via TM and control mice at 1 month of age. Mice were anesthetized (ketamine/xylazine, 100/10 mg/kg, respectively, i.p.) and body temperature was maintained near 38°C with a heating pad. All acoustic stimuli were 5-ms pulses with 0.5-ms linear ramps. Tonal stimuli consisted of 8, 16, and 32 kHz to stimulate the low-, mid-, and high-frequency regions of the basilar membrane. After amplification (Cambridge Audio Azur 540a integrated amplifier), the stimuli were broadcast through a Motorola piezoelectric speaker (model no. 15D87141E02) fitted with a plastic funnel and 2-mm-diameter tubing over the speaker front, producing an acoustic wave guide positioned in the external meatus approximately 0.5 cm from the tympanum. Using continuous tones, stimulus amplitude was calibrated at the end of the tubing with a Bruel and Kjaer 2610 measuring amplifier (fast, linear weighting), 4135 microphone (grid on), and 4230 pistonphone calibrator. All stimulus amplitudes were dB SPL (in reference to 20 µPa). Stimuli were generated (195 kHz sampling rate) and responses digitized (10 kHz sampling rate) using TDT System III hardware and software (BioSig). ABRs were recorded with a 27G subdermal steel electrode (Ambu neuroline subdermal) placed behind the left ear, with indifferent and ground electrodes (steel wire, 30G) placed subcutaneously at the vertex and hindlimbs, respectively. After amplification (60 dB, Grass P511 AC), filtering (0.3 Hz–1 kHz, TDT PF1), and averaging (n = 600–1,024), thresholds ( $\pm$ 6 dB) were determined using a peak discriminator algorithm (ABR Peak Analysis software, v1.5.7.60, EPL) and by visual inspection as the minimum stimulus amplitude that produced an ABR wave pattern similar to that produced for the highest intensity stimulus (90 dB). Data are reported as standard error of the mean (SEM).

**Balance Behavior: BCH Location**

Balance function was assessed using open field observation as described before.<sup>21</sup> The open field test was conducted using a circular frame measuring 42 cm in diameter, placed inside a sound chamber with overhead LED lighting, and set to 30 lux at the center, inside a dimmed room. Mice were placed one at a time inside the circular open field and allowed to explore for 5 min. Behavior was recorded and tracked using EthoVision XT, enabling measures of distance traveled and velocity. Open field assessments were all conducted in a blinded manner.

**Balance Behavior: LSUSHC Location**

Balance behavior was assessed in a 55 (length) × 35 (width) × 38-cm (height) ventilated box and filmed using a video camera connected to an HP computer (Dell, Round Rock, TX, USA). The open field test was performed over 2 min at P21–P25. The number of rotations, defined as the number of times the mouse body completed a 360° angle continuous turn during the 2-min recording, was analyzed using Any-Maze software (Stoelting, Wood Dale, IL, USA).

**RVOR: UMMC Location**

VORs were performed on WT, ASO-29-treated- and untreated-Ush1c<sup>216AA</sup> mice. ASO-29-injected mice were shipped, along with WT and control mice, from the Géléc laboratory. The experiments were done blinded, with the experimenter unaware of the genotype and treatment of the mice being assessed. Rotational VORs were recorded as described previously.<sup>49–51</sup> Briefly, each mouse was implanted with a small head holder on the skull and was allowed 7 days to recover before eye movement tests. Horizontal and vertical eye position signals were recorded using a video-based eye tracking system (ISCAN ETS-200, ISCAN, Burlington, MA, USA). An infrared camera equipped with a zoom lens (Computar TV zoom lens, Computar Optics Group, Japan) was attached to the platform mounted on a servo-controlled rotator/sled (Neurokinetic, Pittsburgh, PA, USA) and was focused on the left eye of each mouse, which was fixed to the platform via the head holder. The eye tracker tracked the pupil center and a reference corneal reflection at a speed of 240 frames/s with a spatial resolution of 0.1 degrees. Calibration was achieved by rotating the camera to the left 10 degrees and to the right 10 degrees around the vertical axis of the eye. Following the calibration, horizontal head rotations were delivered at 0.2, 0.5, 1, 2, and 4 Hz (60 degrees/s peak velocity) to measure the steady-state VOR responses. Signals related to horizontal and vertical eye position and head position were sampled at 1 kHz at 16 bits resolution by a CED Power 1401 system (Cambridge Electronics Devices, Cambridge, UK). Eye movement responses were analyzed using Spike2 (Cambridge Electronics Devices), MATLAB (MathWorks, Natick, MA, USA), and SigmaPlot (Systat Software, San Jose, CA, USA). Eye position signals were filtered and differentiated with a band-pass of DC to 50 Hz to obtain eye velocity signals. Gains and phases of the rotational VORs were calculated by performing a fast Fourier trans-

form (FFT) on the de-saccaded eye velocity signal and head rotation velocity signal.

**Vestibular Afferent Recording: UMMC Location**

Single-unit recording of vestibular afferents was performed under ketamine/xylazine anesthesia as described previously.<sup>49,52,53</sup> Briefly, the head was stabilized on a stereotaxic frame (David Kopf Instruments, Tujunga, CA, USA) via a head holder. Core body temperature was monitored and maintained at 36–37°C with a heating pad (Frederick Haer & Company, Bowdoinham, ME, USA). A craniotomy was performed to allow access of the vestibular nerve by a microelectrode filled with 3 M NaCl (40–60 macrophages) (Sutter Instruments, Novato, CA, USA). Extracellular recording was obtained using a MNAP system (Plexon, Dallas, TX, USA). Every spontaneously active nerve fiber encountered was tested. Each afferent's spontaneous activity was first recorded for calculating the regularity and baseline firing rate. Then, each semicircular canal was brought into the plane of earth-horizontal rotation, and the isolated afferent's response to head rotation along with horizontal and vertical head position signals were recorded. Extracellular voltage signals were sampled with the CED-Micro1401 data acquisition unit (Cambridge Electronic Design Ltd., Cambridge, UK), at 20 kHz with 16-bit resolution and a temporal resolution of 0.01 ms. Head position signals were sampled at 1 kHz. Regularity of vestibular afferents was determined by calculating their normalized coefficient of variation of interspike intervals, i.e., CV\*s. Vestibular afferents were classified as regular (CV\* ≤ 0.1) or irregular (CV\* > 0.1) units based on their CV\*<sup>54–56</sup>. To quantify an afferent's responses to head rotation, the fundamental response was extracted from the averaged data using an FFT analysis. Gains and phases relative to head velocity were calculated at 1 Hz.

**Immunohistochemistry: BCH and LSUHSC Locations**

Fluorescent labeling of microdissected preparations of the organ of Corti was used to study the localization of ASO-29 and the expression of harmonin protein in mutant and heterozygous mice treated with ASO-29 or vehicle (saline) as described previously.<sup>15,16</sup> Temporal bones of 4-week-old mice were excised after euthanasia and fixed in 2–4% paraformaldehyde (PFA) for 1 h. Small perforations were performed at the round and oval windows as well as the apex of the cochlea to facilitate diffusion of the fixative. For tissues from mice treated with ASO-29-fluorescein, after several PBS washes, the temporal bones were decalcified for 24–36 h with 120 mM EDTA. Permeabilization was then performed with 0.01% Triton X-100 for 30 min. Anti-myosin 7A antibodies (1/500, #25–6790, Proteus Bioscience, CA, USA) were used to label hair cells for 24–48 h at room temperature followed by incubation with secondary antibodies (1:200, Alexa Fluor 633 anti-rabbit immunoglobulin G [IgG], Thermo Fisher Scientific) for 2–3 h as described previously.<sup>21</sup> For ASO-29 labeling, anti-ASO (1:250, Ionis Pharmaceuticals) and anti-parvalbumin (1:250, Sigma-Aldrich) antibodies were used to label hair cells overnight at 4°C. In other tissues, permeabilization was performed with 1:1 methanol/acetone for 10 min at –20°C followed by incubation overnight at 4°C first with anti-harmonin-b (1:100, gift from P. Gillespie) antibodies and then with secondary antibodies (1:200, Alexa Fluor 533).

Alexa Fluor 488 phalloidin was used to label F-actin filaments (1:150, Invitrogen) for 1 hour at 4°C. ASO-29-fluorescein images were obtained at the BCH location on a Zeiss LSM 710 laser confocal microscope and processed with a Zeiss LSM image viewer 4.2. ASO-29 and harmonin images were obtained at the LSUHSC location on a Zeiss LSM 710 confocal microscope and processed with ImageJ software.

### Statistical Analyses

Statistical analyses were performed with Origin 2016 (OriginLab). Data are presented as mean  $\pm$  SD or SEM as noted in the text and figure legends. One-way analysis of variance (ANOVA) followed by Tukey and Holm-Sidak (or Bonferroni) *post hoc* analyses were performed to compare selected pairs of means. Two-way ANOVA was used for multiple comparison.

### SUPPLEMENTAL INFORMATION

Supplemental Information can be found online at <https://doi.org/10.1016/j.ymthe.2020.08.002>.

### AUTHOR CONTRIBUTIONS

J.J.L. (organ of Corti) and C.N.-L. (utricle) performed immunohistochemistry. B.P. performed stiff-probe physiology experiments. B.P. performed RWM injections. C.M.T. and K.N.R. performed TM treatments. B.P., C.N.-L., K.N.R., A.G., and A.P. performed ABR, DPOAE, and behavioral experiments. F.M.J. performed RT-PCR and gel electrophoresis experiments. B.P., C.N.-L., and A.G. performed scanning EM. J.H., T.C., H.Z., and W.Z. performed VORs and single-unit vestibular afferent recordings. J.J.L. and G.S.G.G. analyzed immunohistochemistry experiments. J.J.L., B.P., A.P., H.E.F., and G.S.G.G. analyzed physiology experiments. M.L.H. designed and analyzed splicing experiments. H.G. performed injections of the mice sent to UMMC. H.Z., W.Z., J.H., T.C., A.P., H.E.F., and J.J.L. analyzed and interpreted the VORs and single-unit vestibular afferent recordings experiments. J.J.L., A.P., H.E.F., F.R., M.L.H., and G.S.G.G. interpreted the results. C.M.T., A.P., B.P., G.S.G.G., and J.J.L. wrote the manuscript.

### CONFLICTS OF INTEREST

F.R. is an employee of Ionis Pharmaceuticals. M.L.H. receives funding from Ionis Pharmaceuticals. J.J.L. and G.S.G.G. have served as consultants for Decibels Therapeutics. The remaining authors declare no competing interests.

### ACKNOWLEDGMENTS

This work was supported by the National Institutes of Health (grants R01 EY030499, U54 GM104940, and P30 GM103340 [to J.J.L.], R01 DC012060 and R21 DC017293 [to H.Z.], and R01 DC012596 [to M.L.H.]), the Usher 2020 Foundation (to J.J.L.), the Ush One See Foundation (to J.J.L.), and the Barber Gene Therapy Research Fund to BCH (to G.S.G.G.). The Zeiss LSM 710 laser confocal microscope at BCH was supported by NIH IDRC Imaging Core grant P30 HD18655. We thank C. Liberman and K. Hancock (EPL, MEEI) for sharing their ABR Peak Analysis software, and P. Gillespie for gifting the anti-harmonin antibodies.

### REFERENCES

- Boughman, J.A., Vernon, M., and Shaver, K.A. (1983). Usher syndrome: definition and estimate of prevalence from two high-risk populations. *J. Chronic Dis.* 36, 595–603.
- Keats, B.J., and Corey, D.P. (1999). The Usher syndromes. *Am. J. Med. Genet.* 89, 158–166.
- Mathur, P., and Yang, J. (2015). Usher syndrome: hearing loss, retinal degeneration and associated abnormalities. *Biochim. Biophys. Acta* 1852, 406–420.
- Cosgrove, D., and Zallocchi, M. (2014). Usher protein functions in hair cells and photoreceptors. *Int. J. Biochem. Cell Biol.* 46, 80–89.
- El-Amraoui, A., and Petit, C. (2005). Usher I syndrome: unravelling the mechanisms that underlie the cohesion of the growing hair bundle in inner ear sensory cells. *J. Cell Sci.* 118, 4593–4603.
- Kremer, H., van Wijk, E., Märker, T., Wolfrum, U., and Roepman, R. (2006). Usher syndrome: molecular links of pathogenesis, proteins and pathways. *Hum. Genet.* 15, R262–R270.
- Pan, L., and Zhang, M. (2012). Structures of usher syndrome 1 proteins and their complexes. *Physiology (Bethesda)* 27, 25–42.
- Reiners, J., and Wolfrum, U. (2006). Molecular analysis of the supramolecular usher protein complex in the retina. Harmonin as the key protein of the Usher syndrome. *Adv. Exp. Med. Biol.* 572, 349–353.
- DeAngelis, M.M., Doucet, J.P., Drury, S., Sherry, S.T., Robichaux, M.B., Den, Z., Pelias, M.Z., Ditta, G.M., Keats, B.J., Deininger, P.L., and Batzer, M.A. (1998). Assembly of a high-resolution map of the Acadian Usher syndrome region and localization of the nuclear EF-hand acidic gene. *Biochim. Biophys. Acta* 1407, 84–91.
- Keats, B.J., Nouri, N., Pelias, M.Z., Deininger, P.L., and Litt, M. (1994). Tightly linked flanking microsatellite markers for the Usher syndrome type I locus on the short arm of chromosome 11. *Am. J. Hum. Genet.* 54, 681–686.
- Savas, S., Frischhertz, B., Pelias, M.Z., Batzer, M.A., Deininger, P.L., and Keats, B.B. (2002). The *USH1C* 216G  $\rightarrow$  A mutation and the 9-repeat VNTR(t,t) allele are in complete linkage disequilibrium in the Acadian population. *Hum. Genet.* 110, 95–97.
- Lentz, J., Savas, S., Ng, S.S., Athas, G., Deininger, P., and Keats, B. (2005). The *USH1C* 216G  $\rightarrow$  A splice-site mutation results in a 35-base-pair deletion. *Hum. Genet.* 116, 225–227.
- Lentz, J., Pan, F., Ng, S.S., Deininger, P., and Keats, B. (2007). *Ush1c216A* knock-in mouse survives Katrina. *Mutat. Res.* 616, 139–144.
- Lentz, J.J., Gordon, W.C., Farris, H.E., MacDonald, G.H., Cunningham, D.E., Robbins, C.A., Tempel, B.L., Bazan, N.G., Rubel, E.W., Oesterle, E.C., and Keats, B.J. (2010). Deafness and retinal degeneration in a novel *USH1C* knock-in mouse model. *Dev. Neurobiol.* 70, 253–267.
- Lentz, J.J., Jodelka, F.M., Hinrich, A.J., McCaffrey, K.E., Farris, H.E., Spalitta, M.J., Bazan, N.G., Duelli, D.M., Rigo, F., and Hastings, M.L. (2013). Rescue of hearing and vestibular function by antisense oligonucleotides in a mouse model of human deafness. *Nat. Med.* 19, 345–350.
- Ponnath, A., Depreux, F.F., Jodelka, F.M., Rigo, F., Farris, H.E., Hastings, M.L., and Lentz, J.J. (2018). Rescue of outer hair cells with antisense oligonucleotides in usher mice is dependent on age of treatment. *J. Assoc. Res. Otolaryngol.* 19, 1–16.
- Vijayakumar, S., Depreux, F.F., Jodelka, F.M., Lentz, J.J., Rigo, F., Jones, T.A., and Hastings, M.L. (2017). Rescue of peripheral vestibular function in Usher syndrome mice using a splice-switching antisense oligonucleotide. *Hum. Mol. Genet.* 26, 3482–3494.
- Dias, N., and Stein, C.A. (2002). Antisense oligonucleotides: basic concepts and mechanisms. *Mol. Cancer Ther.* 1, 347–355.
- Havens, M.A., and Hastings, M.L. (2016). Splice-switching antisense oligonucleotides as therapeutic drugs. *Nucleic Acids Res.* 44, 6549–6563.
- Rigo, F., Seth, P.P., and Bennett, C.F. (2014). Antisense oligonucleotide-based therapies for diseases caused by pre-mRNA processing defects. *Adv. Exp. Med. Biol.* 825, 303–352.
- Pan, B., Askew, C., Galvin, A., Heman-Ackah, S., Asai, Y., Indzhykulian, A.A., Jodelka, F.M., Hastings, M.L., Lentz, J.J., Vandenberghe, L.H., et al. (2017). Gene therapy restores auditory and vestibular function in a mouse model of Usher syndrome type 1c. *Nat. Biotechnol.* 35, 264–272.

22. Juliano, R.L. (2016). The delivery of therapeutic oligonucleotides. *Nucleic Acids Res.* 44, 6518–6548.
23. Stein, C.A., and Castanotto, D. (2017). FDA-approved oligonucleotide therapies in 2017. *Mol. Ther.* 25, 1069–1075.
24. Wood, M.J.A., Talbot, K., and Bowerman, M. (2017). Spinal muscular atrophy: antisense oligonucleotide therapy opens the door to an integrated therapeutic landscape. *Hum. Mol. Genet.* 26 (R2), R151–R159.
25. Huangfu, M., and Saunders, J.C. (1983). Auditory development in the mouse: structural maturation of the middle ear. *J. Morphol.* 176, 249–259.
26. Lee, J., Nist-Lund, C., Solanes, P., Goldberg, H., Wu, J., Pan, B., et al. (2020). Efficient viral transduction in mouse inner ear hair cells with utricule injection and AAV9-PHP.B. *Hearing Research* 394, <https://doi.org/10.1016/j.heares.2020.107882>.
27. Rüscher, A., Lysakowski, A., and Eatock, R.A. (1998). Postnatal development of type I and type II hair cells in the mouse utricle: acquisition of voltage-gated conductances and differentiated morphology. *J. Neurosci.* 18, 7487–7501.
28. Burns, J.C., On, D., Baker, W., Collado, M.S., and Corwin, J.T. (2012). Over half the hair cells in the mouse utricle first appear after birth, with significant numbers originating from early postnatal mitotic production in peripheral and striolar growth zones. *J. Assoc. Res. Otolaryngol.* 13, 609–627.
29. Staecker, H., Praetorius, M., Baker, K., and Brough, D.E. (2007). Vestibular hair cell regeneration and restoration of balance function induced by math1 gene transfer. *Otol. Neurotol.* 28, 223–231.
30. Golub, J.S., Tong, L., Ngyuen, T.B., Hume, C.R., Palmiter, R.D., Rubel, E.W., and Stone, J.S. (2012). Hair cell replacement in adult mouse utricles after targeted ablation of hair cells with diphtheria toxin. *J. Neurosci.* 32, 15093–15105.
31. Wang, T., Chai, R., Kim, G.S., Pham, N., Jansson, L., Nguyen, D.H., Kuo, B., May, L.A., Zuo, J., Cunningham, L.L., and Cheng, A.G. (2015). *Lgr5*<sup>+</sup> cells regenerate hair cells via proliferation and direct transdifferentiation in damaged neonatal mouse utricle. *Nat. Commun.* 6, 6613.
32. Depreux, F.F., Wang, L., Jiang, H., Jodelka, F.M., Rosencrans, R.F., Rigo, F., Lentz, J.J., Brigande, J.V., and Hastings, M.L. (2016). Antisense oligonucleotides delivered to the amniotic cavity in utero modulate gene expression in the postnatal mouse. *Nucleic Acids Res.* 44, 9519–9529.
33. Wang, L., Kempton, J.B., Jiang, H., Jodelka, F.M., Brigande, A.M., Dumont, R.A., Rigo, F., Lentz, J.J., Hastings, M.L., and Brigande, J.V. (2020). Fetal antisense oligonucleotide therapy for congenital deafness and vestibular dysfunction. *Nucleic Acids Res.* 48, 5065–5080.
34. Borkholder, D.A. (2008). State-of-the-art mechanisms of intracochlear drug delivery. *Curr. Opin. Otolaryngol. Head Neck Surg.* 16, 472–477.
35. Salt, A.N., Ohyama, K., and Thalmann, R. (1991). Radial communication between the perilymphatic scalae of the cochlea. I: Estimation by tracer perfusion. *Hear. Res.* 56, 29–36.
36. Piu, F., and Bishop, K.M. (2019). Local drug delivery for the treatment of neurotology disorders. *Front. Cell. Neurosci.* 13, 238.
37. Mikulec, A.A., Hartsock, J.J., and Salt, A.N. (2008). Permeability of the round window membrane is influenced by the composition of applied drug solutions and by common surgical procedures. *Otol. Neurotol.* 29, 1020–1026.
38. Sadreev, I.I., Burwood, G.W.S., Flaherty, S.M., Kim, J., Russell, I.J., Abdullin, T.I., and Lukashkin, A.N. (2019). Drug diffusion along an intact mammalian cochlea. *Front. Cell. Neurosci.* 13, 161.
39. Nuttall, A.L., Ricci, A.J., Burwood, G., Harte, J.M., Stenfelt, S., Cayé-Thomasen, P., Ren, T., Ramamoorthy, S., Zhang, Y., Wilson, T., et al. (2018). A mechano-electrical mechanism for detection of sound envelopes in the hearing organ. *Nat. Commun.* 9, 4175.
40. Shen, L., Engelhardt, J.A., Hung, G., Yee, J., Kikkawa, R., Matson, J., Tayefeh, B., Machemer, T., Giclas, P.C., and Henry, S.P. (2016). Effects of repeated complement activation associated with chronic treatment of cynomolgus monkeys with 2'-O-methoxyethyl modified antisense oligonucleotide. *Nucleic Acid Ther.* 26, 236–249.
41. Toonen, L.J.A., Casaca-Carreira, J., Pellisé-Tintoré, M., Mei, H., Temel, Y., Jahanshahi, A., and van Roon-Mom, W.M.C. (2018). Intracerebroventricular administration of a 2'-O-methyl phosphorothioate antisense oligonucleotide results in activation of the innate immune system in mouse brain. *Nucleic Acid Ther.* 28, 63–73.
42. Rabinowitz, J., Chan, Y.K., and Samulski, R.J. (2019). Adeno-associated virus (AAV) versus immune response. *Viruses* 11, E102.
43. Vandamme, C., Adjali, O., and Mingozzi, F. (2017). Unraveling the complex story of immune responses to AAV vectors trial after trial. *Hum. Gene Ther.* 28, 1061–1074.
44. Guan, X., and Gan, R.Z. (2011). Effect of middle ear fluid on sound transmission and auditory brainstem response in guinea pigs. *Hear. Res.* 277, 96–106.
45. Dewan, K.K., Taylor-Mulneix, D.L., Campos, L.L., Skarlupka, A.L., Wagner, S.M., Ryman, V.E., Gestal, M.C., Ma, L., Blas-Machado, U., Faddis, B.T., and Harvill, E.T. (2019). A model of chronic, transmissible otitis media in mice. *PLoS Pathog.* 15, e1007696.
46. MacArthur, C.J., Hefeneider, S.H., Kempton, J.B., Parrish, S.K., McCoy, S.L., and Trune, D.R. (2006). Evaluation of the mouse model for acute otitis media. *Hear. Res.* 219, 12–23.
47. Sung, C.Y.W., Seleme, M.C., Payne, S., Jonjic, S., Hirose, K., and Britt, W. (2019). Virus-induced cochlear inflammation in newborn mice alters auditory function. *JCI Insight* 4, 128878.
48. Askew, C., Rochat, C., Pan, B., Asai, Y., Ahmed, H., Child, E., Schneider, B.L., Aebischer, P., and Holt, J.R. (2015). *Tmc* gene therapy restores auditory function in deaf mice. *Sci. Transl. Med.* 7, 295ra108.
49. Stewart, C., Yu, Y., Huang, J., Maklad, A., Tang, X., Allison, J., Mustain, W., Zhou, W., and Zhu, H. (2016). Effects of high intensity noise on the vestibular system in rats. *Hear. Res.* 335, 118–127.
50. Asai, Y., Pan, B., Nist-Lund, C., Galvin, A., Lukashkin, A.N., Lukashkina, V.A., Chen, T., Zhou, W., Zhu, H., Russell, I.J., et al. (2018). Transgenic *Tmc2* expression preserves inner ear hair cells and vestibular function in mice lacking *Tmc1*. *Sci. Rep.* 8, 12124.
51. Nist-Lund, C.A., Pan, B., Patterson, A., Asai, Y., Chen, T., Zhou, W., Zhu, H., Romero, S., Resnik, J., Polley, D.B., et al. (2019). Improved TMC1 gene therapy restores hearing and balance in mice with genetic inner ear disorders. *Nat. Commun.* 10, 236.
52. Zhu, H., Tang, X., Wei, W., Maklad, A., Mustain, W., Rabbitt, R., Highstein, S., Allison, J., and Zhou, W. (2014). Input-output functions of vestibular afferent responses to air-conducted clicks in rats. *J. Assoc. Res. Otolaryngol.* 15, 73–86.
53. Zhu, H., Tang, X., Wei, W., Mustain, W., Xu, Y., and Zhou, W. (2011). Click-evoked responses in vestibular afferents in rats. *J. Neurophysiol.* 106, 754–763.
54. Lasker, D.M., Han, G.H., Park, H.J., and Minor, L.B. (2008). Rotational responses of vestibular-nerve afferents innervating the semicircular canals in the C57BL/6 mouse. *J. Assoc. Res. Otolaryngol.* 3, 334–348.
55. Goldberg, J.M. (1984). Relation between discharge regularity and responses to externally applied galvanic currents in vestibular nerve afferents of the squirrel monkey. *J. Neurophysiology* 51, 1236–1256.
56. Young, E.D., Fernandez, C., and Goldberg, J.M. (1977). Responses of squirrel monkey vestibular neurons to audio-frequency sound and head vibration. *Acta Otolaryngol.* 84, 352–360.